Impact of the Normal Zone Propagations Velocity of High Temperature Superconducting Coated Conductors on Resistive Fault Current Limiters

D. Colangelo and B. Dutoit

***Abstract*—The engineering critical current (I_c) of the high temperature superconducting coated conductors (HTS-CCs), today available on the market, is not a uniform parameter and varies significantly along the length of the conductors. Moreover, commercial HTS-CCs have a low normal zone propagation velocity (NZPV). This property, together with the I_c inhomogeneity, exposes the HTS-CCs to local thermal instabilities. A crucial challenge for the design of resistive fault current limiters (RFCLs) based on HTS-CCs is to avoid the thermal runaway of the conductors, and in this respect the enhancement of the NZPV is a promising solution. In the recent years, several methods have been proposed and many and various techniques are now available to enhance the NZPV. Whichever will be the best technical solution to improve NZPV of HTS-CCs, our aim is to quantify the impact the enhancement of NZPV will have on the design of RFCLs based on HTS-CCs. For this reason, we used numerical models to analyze the effects of the enhancement of NZPV on the limitation performance of a RFCL integrated in a medium voltage (MV) power grid. In this manuscript, we quantify the benefits the enhancement of the NZPV will have on the next generation of HTS-CC-based RFCLs for MV grids.**

***Index Terms*—Power Network Modelling, Fault Current Limiters, High Temperature Superconducting Coated Conductors, Normal Zone Propagation Velocity.**

I. Introduction

DUE to the complexity of the manufacturing processes of REBaCuO-based (RE stands for different rare-earth elements such as gadolinium, ytterbium, yttrium, etc.) high temperature superconducting coated conductors (HTS-CCs), the critical current (I_c) of commercial HTS-CCs varies significatively around the average critical current ($I_{c.av}$) of the tapes [1]. When commercial HTS-CCs are subjected to an applied over-current waveform close to $I_{c.av}$, the weak zones of the conductors (characterized by low I_c) might quench to their resistive state. The applied current is locally diverted to the stabilizer layer of the HTS-CCs and sources of heat are formed by Joule heating effect. Commercial HTS-CCs have low thermal diffusivity and their longitudinal normal zone propagation velocity (NZPV) is extremely low (a few tens of cm/s). As a consequence, the heat dissipation remains localized and tapes are exposed to thermal instability.

Manuscript received X Month 2014.

Corresponding author's e-mail: daniele.colangelo@epfl.ch.

D. Colangelo and B. Dutoit are with École polytechnique fédérale de Lausanne, EPFL-SCI-IC-BD , Station 14, 1015 Lausanne, Switzerland.

The research leading to these results has received funding from the European Union Seventh Framework Programme (FP7/2007 - 2013) under grant agreement No. 241285

A common method to reduce the heat generated near the weak zones of the HTS-CCs and to mitigate the local thermal instability, is to increase the thickness of the stabilizer material [2]. The resistance of the stabilizer is lowered, the transport current is rapidly diverted to the stabilizer layer and the heat diffuses faster within the tape. Unfortunately, this solution decreases the series normal state resistance of the HTS-CCs and therefore, when HTS-CCs are used for RFCL purposes, tapes of longer length are required to achieve a given current limitation. A direct consequence is an important increase of the final cost of the device.

An alternative approach to guarantee the local thermal stability is the enhancement of the NZPV of the HTS-CCs. Although the enhancement of the NZPV does not solve the I_c inhomogeneity issues, it helps to propagate the normal zones from the sectors where I_c is lower to the contiguous zones where I_c is higher. Consequently, the power peak densities within the HTS-CCs are sensibly reduced without changing the thickness of the stabilizer layer. In the last years, the enhancement of the NZPV has been extensively studied [3]–[7] and several valid methods have been proposed. Even though, the proposed methods are profoundly different, the common conclusion is that the enhancement of NZPV will represent an important breakthrough for superconducting devices, and in particular for the design of RFCLs.

The discussion on the different techniques to improve NZPV is beyond the scope of our work. The aim of our research is to clarify and to quantify the impact the NZPV enhancement will have on the design of RFCLs. For this reason, we employed our experience in numerical modelling to analyze the impact the increase of the NZPV will have on the design of RFCLs based on HTS-CCs. First, we have modified numerically the NZPV of HTS-CC candidates. All the HTS-CC candidates have the same architecture (similar to the tapes produced by SuperPower inc). Then, we simulated a RFCL designed with HTS-CCs with enhanced NZPV in a busbar coupler configuration. The simulated RFCL has the same specifications of the device developed within the framework of the European project ECCOFLOW [8].

In the current manuscript, we detail the numerical model we used to evaluate the HTS-CC candidates with enhanced NZPV. Afterwards, we report the analysis of the limitation performance of a RFCL for MV power grids designed with HTS-CCs with different NZPVs. We follow with a discussion on the simulation results on the impact the enhancement of

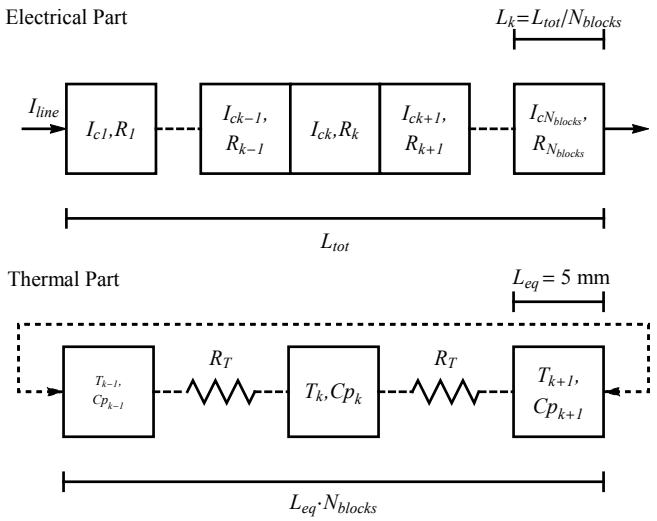

Fig. 1. A schematic overview of the electrical and the thermal part of the numerical model. In the electrical part, the longitudinal length of each tape (L_{tot}) is divided in k blocks of length L_k. The thermal part of the model is solved considering a limited portion of tapes equal to $L_{eq}\cdot N_{blocks}$ and the solution is repeated along the whole length L_{tot}. The thermal conduction between the different part of the tape is implemented through the thermal resistance R_T. Each block implements the same cross-section architecture.

NZPV will have on the design of HTS-CC-based RFCLs.

II. Overview of the numerical model

Each phase of a RFCL device is composed by as many parallel HTS-CCs as needed to obtain the required total critical current ($I_{c.tot}$). Nevertheless, for simplicity, our model does not consider differences between the paralleled HTS-CCs and, therefore, a single HTS-CC is simulated. As shown in Fig. 1, for the electrical part of the model, the longitudinal length of each paralleled tape (L_{tot}) is divided in N_{blocks} isothermal series blocks.

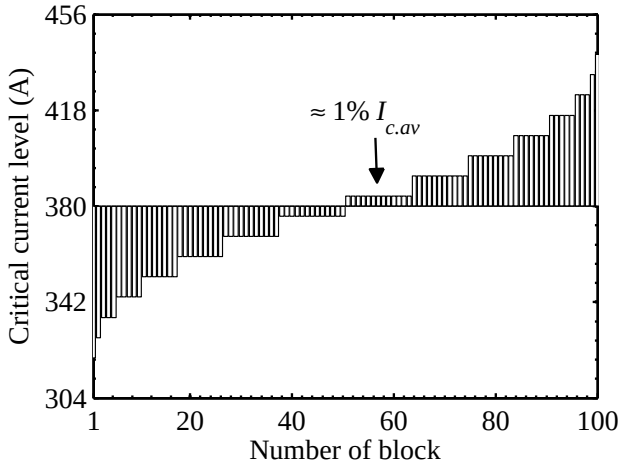

Fig. 2. Critical current levels implemented in the simulated HTS-CCs. The discrete array of I_c levels derives from a Gaussian distribution characterized by an average critical current of circa 380 A and a standard deviation over length of 6.59%.

The model enables us to consider Gaussian distributions of I_c derived from experimental measurements. The Gaussian distribution we considered in our example is characterized by an average value of 380 A and a standard deviation over length (σ) equal to 6.59%. As explained in details in our previous work [9], the array of critical current levels (G1) that represents the Gaussian distributions of I_c takes into account the critical current levels and their corresponding probability. In our example, the Gaussian distribution is discretized in 16 levels of I_c, and the probability assigned to each I_c level is given by the number of blocks with the same level of I_c (Fig. 2)

Even if in principle, it is possible to implements any number of blocks we limited N_{blocks} to 100. With higher N_{blocks} the computation time becomes extremely important and therefore the value we chose is a compromise between the accuracy (on the discretization of the Gaussian distributions of I_c) and an acceptable computation time. Due to the thermal calibration of the model, for the thermal part, the length of each block is fixed to L_{eq} = 5 mm. As in real applications a single HTS-CC is between 100 and 300 m, this would imply a number of blocks larger than 20000. In order to limit N_{blocks} to 100, we calculate the thermal conduction dynamics in a reduced part of the tape and we assume that this part is periodically repeated along the whole tape length L_{tot}. As the number of blocks is fixed to 100, whichever is L_{tot}, the thermal part of the model is solved on 50 mm and repeated for the whole L_{tot}.

The heat exchanged by two adjacent portions of the simulated tape (blocks) is taken into account through the thermal resistance R_T (Fig. 1). The model does not consider the heat exchange between the HTS-CC and the liquid nitrogen bath (adiabatic assumption) where the tape is immersed. Furthermore, the layers of the HTS-CC simulated by the model are: the substrate (hastelloy C-276), the superconducting material and the stabilizer (silver layer) [10]. The buffer layer is then neglected.

The model is developed in Simulink® environment and can be interfaced with common circuit elements. It can be customized for any type of HTS-CC but the calculations presented in the current manuscript are performed using specific characteristics of 12 mm wide HTS-CCs manufactured by SuperPower Inc. More details about the numerical model are reported here [11].

A. A formulation of the power index temperature dependence

The onset of the transition to the normal state of the superconducting material, can be modeled using a phenomenological power law which derives from current-voltage measurements [12]. The power law describes the macroscopic effects of a superconducting material far below I_c and, in principle, it loses validity when the applied current exceeds the critical current of the tape [13]. However, implementing a variable power index (n-value) makes possible to use it to describe the superconducting transition in over-current regimes and, eventually, to the normal state regime [14].

In this respect, we used a particular form of the power law where we defined a variable n-value to model the resistivity

transition of the superconducting material. We model the normal state resistivity (ρ_{norm}) of the superconducting material using data taken from the literature [15]. The whole superconducting to normal state resistivity of the superconducting material is given by

$$\rho_{sc} = \begin{cases} \frac{E_c}{J_c(T)} \left(\frac{|J_{sc}|}{J_c(T)} \right)^{(n(T)-1)}, & T < T_c \\ \rho_{norm}(T), & T \geq T_c \text{ or } \rho_{pl} \geq \rho_{norm} \end{cases} \quad (1)$$

where E_c is an electrical field criterion equal to 1 μV/cm, J_{sc} is the current density through the superconducting material, J_c and n are, respectively, the critical current density and the power index of the modelled HTS-CC. The critical current density J_c decreases linearly with the temperature increase and it corresponds to the transport current (I_{sc}) divided by the superconductor cross-section.

$$J_c(T) = J_c(T_0)\left(\frac{T_c - T}{T_c - T_0}\right), \quad T < T_c \quad (2)$$

where T_0 is the temperature of the cooling bath far from the sample (77 K at 1 atm) and T_c is the critical temperature of the tape (≈ 92 K). The empirical temperature dependence of the transition index we implement in our numerical model is the following one

$$n = \begin{cases} k1\left[\frac{\chi T_0 - T}{\chi T_0 - T_0} + 1\right] + 1, & T \leq \chi T_0 \\ k1\left(\frac{T_c - T}{T_c - \chi T_0}\right)^{\beta} + 1, & \chi T_0 < T \leq T_c \end{cases} \quad (3)$$

where the value β determines the shape of the temperature dependence of the n-value. The parameters $k1$ is equal to $(n_0 - 1)/2$ where n_0 is the average transition index obtained from the producer datasheet.

As shown in Fig. 3, the temperature dependence is divided in three regimes. In the first regime, the dissipation of power is extremely low and the n-value varies linearly with the temperature [16]. The parameter χ defines the transition between the first and the second regime of the characteristic. As soon as the losses become important ($T > \chi T$), the function switches to the second regime and the transition index falls down from circa half of its initial value to 1 [17]. In our case, the parameter β is equal to 0.25 that is a common value used to model the over-current resistivity transition to normal state [18], [19].

We faced our model against four points over-current measurements. A sinusoidal voltage drop of 600 V (peak) was applied to a HTS-CC of 8 m of length and the transport current was set through a variable resistance in series to the tape. The measures were performed at Karlsruhe Institute of Technology (KIT) and shared in the framework of the ECCOFLOW project. Two examples of comparison between the model and experimental measurements are shown in Fig. 4a-b. The limited current (blue solid line in Fig. 4a-b) measured during the experiences, is used as input in the numerical model. In the two examples (where the limited current is different), with our

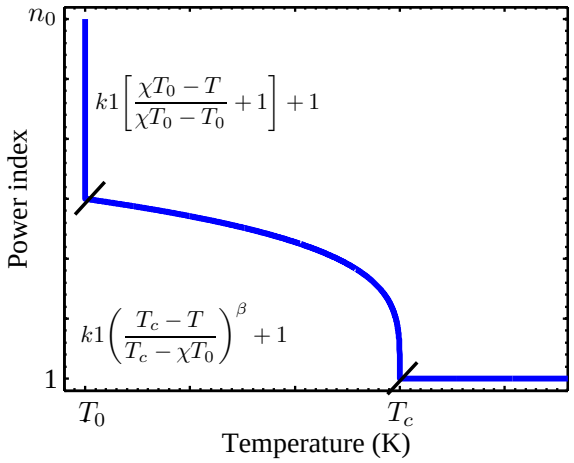

Fig. 3. The temperature dependence of the transition index implemented in the numerical model. The power index decreases with the temperature and it tends to 1 approaching T_c. The initial value of the power index is equal to 31 and β is equal to 0.25.

implementation of the temperature dependence of the power index, the simulated voltage drop across the total length of the HTS-CC (black dashed line in Fig. 4a-b) reproduces with good agreement the voltage drop measured in the experiments (red dotted line in Fig. 4a-b). The thickness of the composite materials of the simulated HTS-CC are respectively, 104.5 μm, 1 μm and 4.8 μm for the substrate, the superconducting material and the stabilizer layer.

B. Thermal conduction and estimation of the NZPV

The heat shared between the different blocks of the simulated HTS-CC is modeled through a thermal resistance (R_T) proportional to the thermal conductivity of the tape. The equivalent resistance R_T comes from the paralleled thermal resistances of the different layers that compose the HTS-CC. The R_T is modelled as follows

$$R_T = \frac{1}{\alpha_{NZPV}} \cdot \sum_{j=1} \frac{L_{th}}{k_j(T) \cdot A_j} \quad (4)$$

where k_j and A_j are, respectively, the thermal conductivity and the cross section of the j_{th} layer of the block k [20], [21].

The parameter L_{th} is needed in order to have a consistent (in term of unit) R_T inversely proportional to both the thermal conductivity and the cross-section of the tape.

The value of R_T (L_{th}) is determined facing the model we developed in Simulink® (lumped element model) against an equivalent model based on finite element method (FEM) techniques. If we consider the superconducting layer as a homogenous material and we consider only the longitudinal gradient of temperature, we can calculate the rate of heat conduction between two generic point solving the Fourier's law in its one-dimensional form.

This easy concept can be scaled to our lumped element model. In the FEM model, the temperature in center of the superconducting layer is recorded with virtual probes each

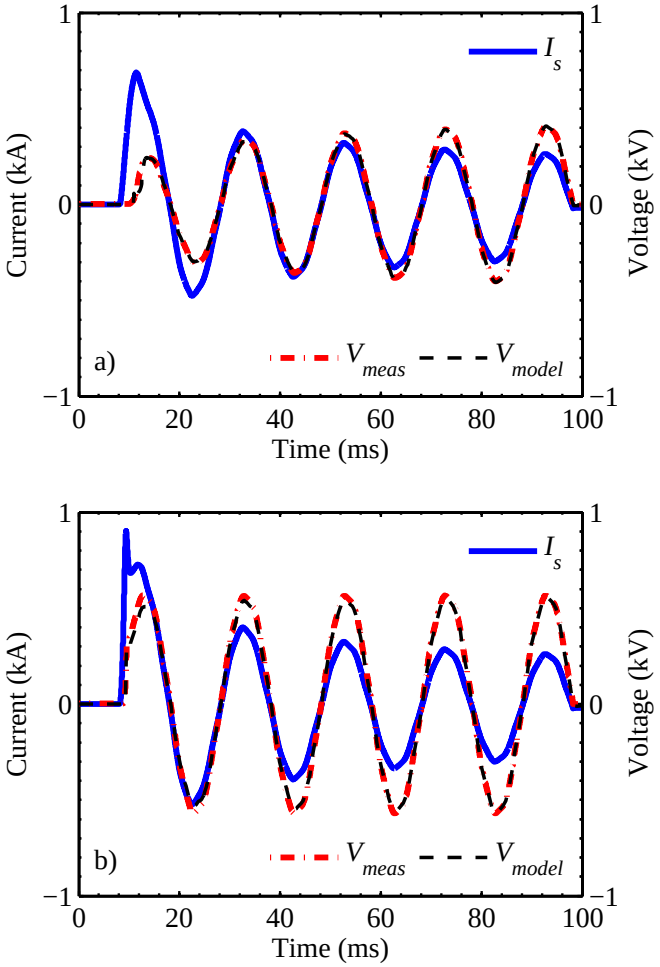

Fig. 4. Comparison between the numerical model and experimental measurements. The measured transport current (I_s) is applied as input to the model. In both cases, where the applied current is different, with our formulation of the temperature dependence of the power index, the model reproduces (V_{model}) the experimental voltage drop (V_{meas}) with good approximation.

5 mm. In our lumped element model, we assume that the temperature of each block is an average temperature equal to the local temperature tracked by a corresponding virtual probe in the FEM model. The value of L_{th} is the value that minimize the error between the FEM model and the lumped element model. The details of the calibration of the thermal part of the model are reported here [11].

The thermal resistance R_T can be varied through the parameter α_{NZPV}. In our model, the variation of α_{NZPV} corresponds to a modification of the heat exchange between the blocks. For different values of α_{NZPV}, the NZPV is calculated simulating an over-current pulse as input of the model. The simulated HTS-CC is divided in 100 blocks and, as shown in Fig. 5, the quench is initiated assigning a lower value of I_c to the middle blocks.

The voltage drops across the different blocks can be easily recorded and the NZPV immediately calculated. The example of Fig. 6 illustrates the time evolution of the voltage drops of block 67, block 68 and block 69 (B67, B68 and B69

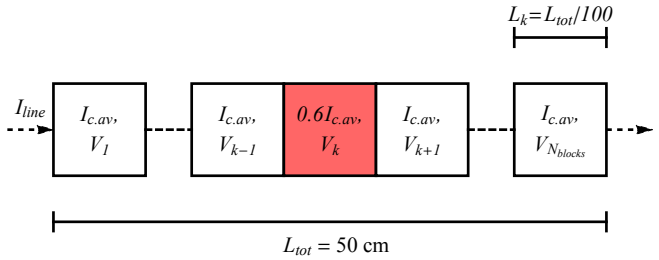

Fig. 5. Sketch of the I_c inhomogeneity distribution used to calculate the NZPV as a function of the parameter α_{NZPV}. The simulated HTS-CC is divided in 100 blocks and the total length of the simulated HTS-CC (L_{tot}) is 50 cm. The length of a single length (L_k) is 5 mm.

in Fig. 6) obtained with a current pulse of $1.2I_{c.av}$. The thickness of the composite materials of the simulated HTS-CC are respectively, 104.5 µm, 1 µm and 4.8 µm for the substrate, the superconducting material and the stabilizer layer. The NZPV of each HTS-CC candidates can be calculated using the following expression

$$NZPV = \frac{L_k}{t_2 - t_1} = \frac{0.5}{t_2 - t_1} \tag{5}$$

where L_k is the length of block k equal, in this particular case, to 5 mm for each block. The relevant times t_1 and t_2 are defined using an arbitrary quench criterion (Fig. 6).

Figure 7 shows the relation between the parameter α_{NZPV} and the resulting NZPV. The NZPV varies sensibly with the thickness of the stabilizer layer (th_{Ag}) because with thinner th_{Ag} the tape is more resistive (in normal state) and, with a fixed current source, higher is the power dissipated within the tape. With α_{NZPV} = 1 and a current pulse of $1.2I_{c.av}$, the NZPV is circa 20 cm/s for th_{Ag} equal to 1.5 µm. Varying the thermal resistance R_T, through the parameter α_{NZPV}, the NZPV is numerically modified starting from actual NZPV of the commercial HTS-CCs (tens of cm/s).

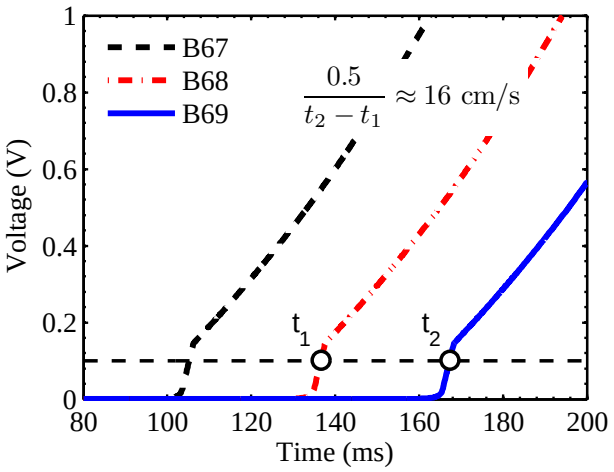

Fig. 6. Evolution of the simulated voltage tracks with a stabilizer layer of 4.8 µm thick, α_{NZPV} = 1 and using as input a current pulse of $1.2I_{c.av}$. The estimated NZPV of the simulated HTS-CC is ≈ 16 cm/s.

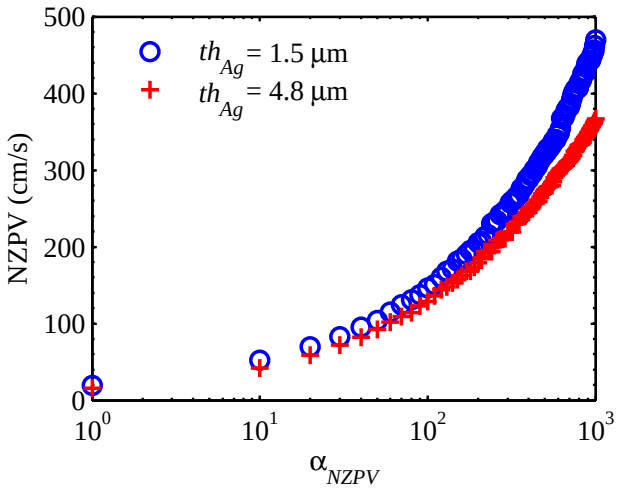

Fig. 7. Relation between the parameter α_{NZPV} and the simulated normal zone propagation velocity for given thickness of stabilizer layer and an applied current pulse of $1.2I_{c.av}$. With th_{Ag} = 1.5 µm the initial NZPV is ≈ 20 cm/s

III. Analysis of the NZPV enhancement

We have simulated a three phases RFCL module with 5 parallel HTS-CCs per phase. The simulated RFCL has the same specifications as the limiter developed within the European project ECCOFLOW. Similarly to our previous work [22], the RFCL is integrated into a MV grid where it operates in busbar coupling configuration. The MV grid is characterized by the real parameters of a HV/MV substation operated by the Spanish utility company Endesa [23] on the Balearic island of Mallorca. Our simulation reproduces not only the ECCOFLOW device but also the grid conditions where the device will be tested.

The single line diagram of the RFCL device integrated in the Endesa substation is shown in Fig. 8. The prospective short-circuit current (I_{pssc}) can be set through a fault resistance

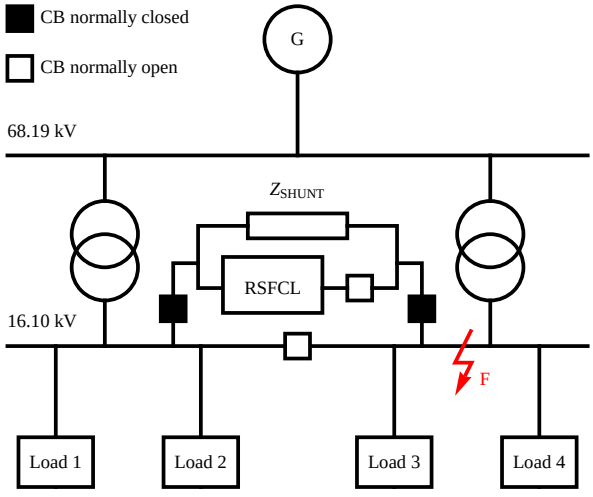

Fig. 8. Single line diagram of the busbar coupling application of the modelled RFCL device. The diagram shows the short-circuit location (F). The modelled RFCL device has the same specifications and the same grid conditions of the ECCOFLOW prototype.

(R_F) inserted in the fault location (point F in Fig. 8). The specifications of the limiter are summarized in Table I.

TABLE I
Fault current limiter parameters

Parameter	Expression	Description
U_0	24 kV	Nominal voltage
$I_{n,RMS}$	1 kA	Nominal current
$I_{c.tot}$	1.9 ± 0.2 kA	Total critical current
Z_{shunt}	1.4 Ω	External shunt impedance
$t_{CB_{HTS}}$	80 ms	CB_{HTS} tripping time
t_{fault}	1 s	Maximum fault time
T_{max}	360 K	Max temperature allowed

In order to avoid the local thermal instability of the HTS-CCs, the ECCOFLOW prototype was manufactured using tapes 180 m long (length of a single tape per phase, L_{tot}) and stabilized with an equivalent silver layer thickness (th_{Ag}) of 3.5 µm.

In the simulations reported in this manuscript, the thickness of the silver stabilizer is fixed to 1.5 µm and the length of the paralleled HTS-CCs (length of a single tape per phase) is chosen in order to have the same resistance offered by a tape with L_{tot} = 180 m and th_{Ag} = 3.5 µm.

For any thickness of stabilizer, it is easy to obtain the resistance per unit of length (R_{pul}). Then, it is possible to estimate the equivalent resistance, offered by a HTS-CC during the limitation of a short-circuit (R_{int}), integrating R_{pul} (Fig. 9) over the interval of temperature as follows

$$R_{int} = \frac{1}{T_{max} - T_c} \int_{T_c}^{T_{max}} R_{pul}(T) dT \qquad (6)$$

where T_{max} is the maximum admissible temperature (360 K). Afterwards, it is extremely simple to calculate which L_{tot} gives the same resistance given by L_{tot} = 180 m and th_{Ag} = 3.5 µm. In the case of th_{Ag} = 1.5 µm, we obtain a single tape per phase equal to 100 m. Keeping fixed th_{Ag} = 1.5 µm and L_{tot} = 100 m, we varied numerically the NZPV of HTS-CCs from ≈ 20 cm/s up to ≈ 500 cm/s. The summary of the performed simulations is reported in Table II.

TABLE II
Summary of the simulation parameters

Parameter	Value	Description
th_{Ag}	1.5 µm	Thickness silver stabilizer
L_{tot}	100 m	Length of a single HTS-CC
$NZPV$	from ≈ 20 up to ≈ 500 cm/s	Normal zone prop. velocity

A. Tape with low NZPV

The I_{pssc} on the busbar line is set varying the fault resistance R_F at the short-circuit location F (Fig. 8). When the fault is simulated with relatively high value of R_F (low values of I_{pssc}), the zones/blocks of the simulated HTS-CC that are characterized by low I_c quench and limit the short-circuit current through the device.

In case of low silver stabilization (e.g. th_{Ag} = 1.5 µm), the few quenched zones will introduce in the grid their resistance

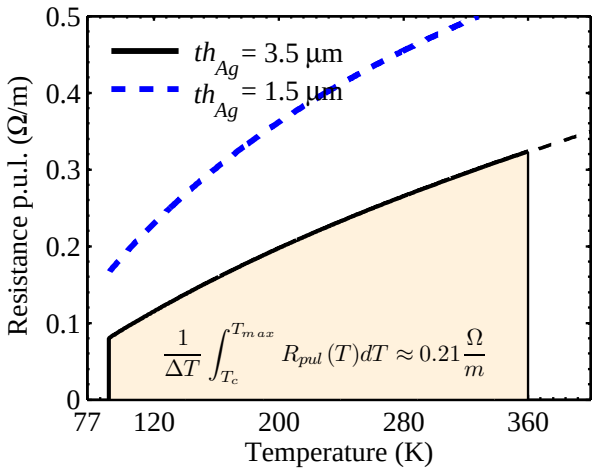

Fig. 9. Normal state resistance per unit length of a HTS-CC in case of a stabilizer thickness of 3.5 µm (solid black line) and a stabilizer thickness of 1.5 µm (dashed blue line). In the range between T_c and T_{max}, the R_{pul} is used to calculate the L_{tot} of the simulated HTS-CCs.

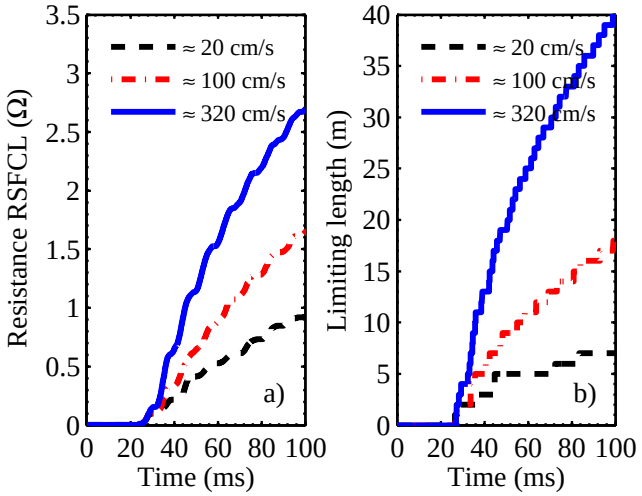

Fig. 10. Resistance profile of the device (a) and limiting length of a single HTS-CC (b) with R_F = 2 Ω and a stabilizer thickness of 1.5 µm. The portion of tape involved in the limitation of the fault current L_{lim} is proportional to the NZPV of the tape.

(black dashed line of Fig. 10a) and the limited current through a single parallel HTS-CC might fall below $I_{c.av}$.

As in this case the HTS-CCs are characterized by low NZPV, the heat developed in the quenched parts of the tapes by Joule heating effect does not evacuate and the zones with higher I_c do not contribute to the limitation of the fault.

As a consequence, the short-circuit current is limited by a small portion of the paralleled HTS-CCs (black dashed curve of Fig. 10b) and the temperature increase is mainly hindered by the heat capacity of the quenched portions of the HTS-CCs (limiting length, L_{lim}). If the amount of the HTS-CCs involved in the limitation of the fault is too small, in some points of L_{lim} the temperature could exceed 360 K before the intervention of protection circuit breaker (80 ms in our simulations). The evident consequence is the local thermal instability of the parallel HTS-CCs of the RFCL module.

B. Tape with enhanced NZPV

The NZPV has no influence on the I_c inhomogeneity. Therefore, under low value of I_{pssc}, even with higher NZPV, the zones of the HTS-CCs characterized by low critical current ($I_c < 0.9 I_{c.av}$) will quench limiting the fault current through the paralleled tapes. Unlike the previous case (low NZPV), the heat developed in the sectors quenched to the normal state propagates to the contiguous zones with higher I_c. The total resistance of the RFCL is higher (red dashed line and blue solid line of Fig. 10a) but the portion of tape which is involved in the limitation of the fault current is now much longer (red dashed line and blue solid line of Fig. 10b). A higher heat capacity contributes to the limitation of the fault current. The amount of energy released locally during the fault is lower than the maximum energy the tape can withstand.

As shown in Fig. 11, with R_F = 0, the maximum admissible temperature criterion is respected independently by the NZPV of the HTS-CC candidates. Extending the analysis to $R_F >$ 0 and keeping the parameter α_{NZPV} = 1 (corresponding to a NZPV ≈ 20 cm/s), it is evident that HTS-CCs, 100 m long with th_{Ag} = 1.5 µm, are subjected to local thermal instability and a dangerous range of possible I_{pssc} is left (black dashed line of Fig. 11). Instead, the local stability of such HTS-CCs can be achieved improving the NZPV. With a NZPV grater than 320 cm/s, the final temperature of the tapes is below 360 K and the local thermal stability is extended to low values of I_{pssc} (blue solid line of Fig. 11).

IV. Conclusion

The aim of this research is to investigate what will be the impact of the enhancement of the NZPV of HTS-CCs on the design of RFCLs for MV power grids. We have modified numerically the NZPV of potential HTS-CC candidates for

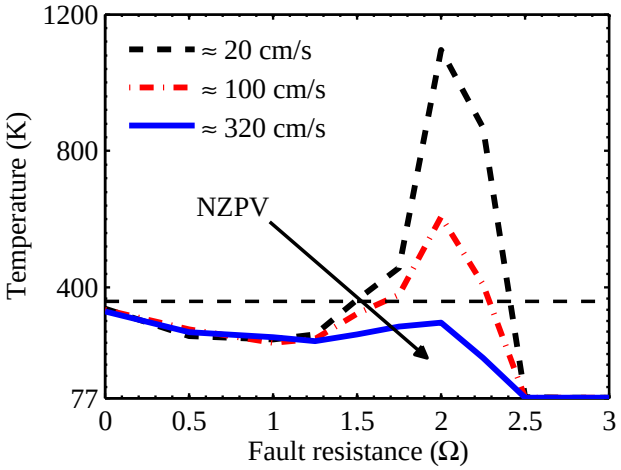

Fig. 11. Final temperature of the weakest zone of the tape function of the fault resistance R_F. With a current inhomogeneity distribution G1 and th_{Ag} = 1.5 µm, a NZPV of 320 cm/s can guarantee the thermal stability for the whole range of short-circuit currents.

RFCL applications keeping fixed the thickness of the stabilizer and the length of the tape. Then, we have used our experience in numerical modelling to analyzed the performance of a RFCL with the same specifications of the device developed in the framework of the ECCOFLOW project. The local thermal stability of the HTS-CCs of the ECCOFLOW prototype was achieved designing the limiter with tapes 180 m long, stabilized with a thick stabilizer layer of 3.5 μm and a NZPV in the order of few tens of cm/s (value of the actual commercial HTS-CCs). The choice of a thick stabilizer is extremely conservative and provides the needed thermal stability but, at the same time, tapes of long length are required to achieve a given current limitation. A higher NZPV will not solve the I_c inhomogeneity of the HTS-CCs but it will enable us to design the next generation of RFCLs with less stabilized HTS-CCs, and consequently shorter tapes. With our numerical model, we can quantify the real impact of NZPV on the design of RFCLs. For instance, with a NZPV greater than 320 cm/s, the amount of HTS-CCs needed for the safe design of RFCLs, with the characteristics of the ECCOFLOW prototype, could be reduced of the 40%. We believe the confirmation of such results and the implementation of techniques able to enhance the NZPV on the manufacturing processes of 12 mm wide HTS-CCs, will represent an important breakthrough in the design of RFCLs for MV applications.

REFERENCES

[1] SuperPower.inc FCL Application SuperPower 2G HTS Wire Spec Sheet [Online]. http:\\www.superpower-inc.com.

[2] Fu Y., Tsukamoto O. and Furuse M., "Copper stabilization of YBCO coated conductor for quench protection", $IEEE\ Trans.\ Appl.\ Supercond.$, vol. 13, no. 2, pp. 1780-1783, Jun. 2003.

[3] Badel A. et al., "Hybrid model of quench propagation in coated conductors for fault current limiters", $Supercond.\ Sci.\ Technol.$ vol. 25 art. no. 095015, 2012.

[4] Antognazza L. et al., "Comparison between the behavior of HTS thin film grown on sapphire and coated conductors for fault current limiter applications", $IEEE\ Trans.\ Appl.\ Supercond.$, vol. 19, no. 3, pp. 1960-1963, Jun. 2009.

[5] Roy F. et al., "Numerical studies of the quench propagation in coated conductors for fault current limiters," $IEEE\ Trans.\ Appl.\ Supercond.$, vol. 19, no. 3, pp. 2496-2499, Jun. 2009.

[6] Lacroix C. et al., "Normal zone propagation velocity in 2G HTS coated conductor with high interfacial resistance", $IEEE\ Trans.\ Appl.\ Supercond.$, vol. 23, no. 3, 2013.

[7] Levin G. A., Novak K. A., and Barnes P. N., "The effects of superconductor-stabilizer interfacial resistance on the quench of a current carrying coated conductor", $Supercond.\ Sci.\ Technol.$, vol. 23, no. 1, p. 014021, Jan. 2010.

[8] ECCOFLOW website [Online]. http://www.eccoflow.org.

[9] Colangelo D. and Dutoit B., "Inhomogeneity Effects in HTS Coated Conductors Used as Resistive FCLs in Medium Voltage Grids", $Supercond.\ Sci.\ Tech.$, vol. 25, 095005, 2012.

[10] Park D.K. et al.,"Experimental and numerical analysis of high resistive coated conductor for conceptual design of fault current limiter", $Cryogenics$, vol. 49, no. 6, pp. 249-253, 2009.

[11] Colangelo D. , "Modelling of 2G HTS coated conductors for fault current limiter applications", pp. 28-31, Ph.D. Thesis EPFL 5916, Lausanne, 2013.

[12] Zeldov E. Amer N.M. Koren G. Gupta A. and McElfresh M.W. and Gambino, "Flux creep characteristics in high-temperature superconductors" *Appl. Phys. Lett.*, vol. 56 no. 7, pp. 680-682, 1990.

[13] Brandt H. E., "Superconductor disks and cylinders in an axial magnetic field. I.Flux penetration and magnetization curves", *Phys. Rev. B* vol. 58 no. 10, pp. 6506-6522. 1998.

[14] Paul W. et al., "Fault current limiter based on high temperature superconductors - Different concepts, test results, simulations, applications", *Physica C*, vol. 354, no. 1-4, pp. 27-33, 2001.

[15] Lortz R. et al., "On the origin of the double superconducting transition in overdoped YBa2Cu3Ox", $Physica\ C$, vol. 434, pp. 194-198, 2005.

[16] Berger K. et al., "Influence of temperature and/or field dependences of the E-J power law on trapped magnetic field in bulk YBaCuO", $IEEE\ Trans.\ Appl.\ Supercond.$, vol. 17, no. 2, June 2013.

[17] Angeli G *et al.*Electrical and Thermal Characterization of Commercial Superconducting YBCO Coated Conductors *IEEE Trans. Appl.* vol. 23 no. 6602304, 2013.

[18] Lacroix C. and Sirois F., "Concept of a current flow diverter for accelerating the normal zone propagation velocity in 2G HTS coated conductors", *Supercond. Sci. Technol.*, vol. 27, no. 3, 2014.

[19] Roy F., "Modelling and characterization of coated conductors applied to the design of superconducting fault current limiters", pp. 42-43, Ph.D. Thesis EPFL 4721, Lausanne, 2010.

[20] Handbook of Chemistry and Physics, 12-42, [Online]. http://www.hbcpnetbase.com

[21] Lu J, Choi E S and Zhou H D 2008 Physical properties of Hastelloy® C-276^{TM} at cryogenic temperatures *J. Appl. Phys.* 103 064908

[22] Colangelo D. and Dutoit B., "MV power grids integration of resistive fault current limiter based on HTS-CCs", $IEEE\ Trans.\ Appl.\ Supercond.$, vol. 23 no. 3 art. no. 6378404, 2013.

[23] Endesa website [Online] Available: http://www.endesa.com.